THE VARIATION OF CRITICAL PIPELINE TRENCH BACK-FILL PROPERTIES

Dr Malcolm Bolton and Mr Andrew Barefoot
(mdb@eng.cam.ac.uk)
Cambridge University Engineering Department
Trumpington Street, Cambridge CB2 1PZ, UK

1 Background

The chosen application for this discussion is the resistance which can be offered to the upheaval buckling of pipelines. The total downward vertical force resisting upward pipe buckling can be separated into the effective weight of the pipe W′ (weight per unit length minus the weight of the fluid it displaces), and the soil uplift resistance P. For pipelines with shallow burial (H/D < 6) the soil uplift resistance may usefully be written:

$$P / (\gamma'.H.D) = 1 + 0.1\,(D/H) + F\,(H/D) \qquad (1)$$

where P = uplift resistance
H = height of cover
D = outside diameter of pipe
F = uplift shear factor
γ' = effective unit weight of soil (rate of increase of effective stress with depth in the soil cover).

Equation (1) is generated by assuming a simple sliding block uplift failure mechanism: see Fig 1. This mechanistic approach will tend to overestimate the true uplift resistance, since the actual failure mechanism need not be that shown; observed uplift failures of shallow pipes conform reasonably well, however. An average shear strength τ_{ave} is assumed on the sides of the soil block riding on the pipe.

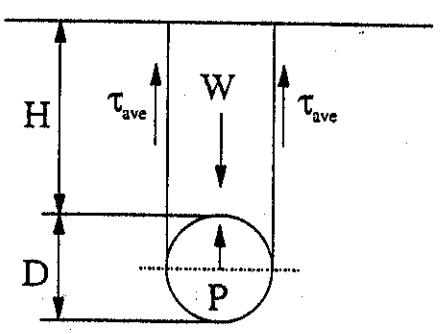

Fig 1 Simple uplift failure mechanism

The first term on the right hand side of equation (1) represents the weight of the rectangle of soil above the crown, the second term represents the weight of the two small off-cuts of soil above the pipe mid-line and below the crown, and the third term represents the effect of the

shear strength τ_{ave} of the soil acting over the depth to the pipe mid-line. By resolving vertically, and comparing with (1), we obtain:

$$F = 2\,(\tau_{ave} / \gamma H)\,\frac{\left(H + \frac{D}{2}\right)}{H} \qquad (2)$$

2 The strength of soil

Soil comprises grains and voids. It may either be regarded as a single-phase material, or as a composite material for which the stresses in the grains and the voids are dealt with separately.

2.1 Single-phase idealisation: cohesion

The shear strength c of a mixed material like concrete or epoxy cement is usually quoted as a given "cohesive" strength which is the maximum possible shear stress which can be induced:

$$c = \tau_{max} \qquad (3)$$

It is recognised that c will depend on the particular mixture, and in the case of soil it is found that the voids ratio (volume of voids per unit volume of solids) is of first importance:

$$c = f(e) \qquad (4)$$

though more careful inspection reveals that pre-consolidation pressure and rate of shearing also have some influence. Unlike concrete, the voids in soil are not fixed in place; water can move and voids can collapse or expand. This is such a strong feature that engineers have become uncomfortable using the cohesive material model for soil except with fully saturated uniformly fine-grained clayey soils in the short term, when relative impermeability keeps the voids ratio constant. This is delivers the "undrained strength" of a clay, given the symbol c_u.

2.2 Dual-phase idealisation: friction

Modern composite materials such as fibre-reinforced plastic, are often treated as dual-phase with the contributions of their components first considered separately and then superimposed. This echoes Terzaghi's earlier treatment of soil as a two-phase material with separable "effective stresses" (σ', τ') carried by the aggregate skeleton, and "pore pressures" u in its voids. In this view, "total stresses" (σ, τ) due to gravity can decomposed thus:

$$\begin{aligned} &\text{normal stress} \quad \sigma = \sigma' + u \\ &\text{shear stress} \quad \tau = \tau' \end{aligned} \qquad (5)$$

The simplest idealisation of the shear strength of a granular aggregate is in terms of the angle of internal friction ϕ, where

$$\tan \phi = (\tau / \sigma')_{max} \qquad (6)$$

but it has to be recognised that internal friction depends not only on inter-particle friction but also on the degree of particle interlocking. Interlocking leads both to dilatancy (increase of volume of the aggregate as previously interlocked particles over-ride) and correspondingly to an extra component of internal angle of friction $\Delta\phi$.

Consider a regular array of rollers which are forced to shear along a macro slip surface SS, but which actually make contact with each other on micro tangents T.

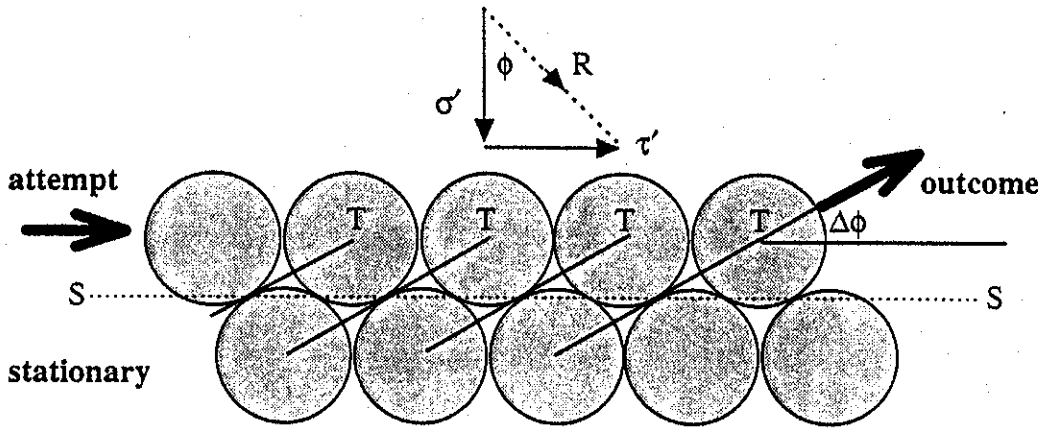

Fig 2 Soil dilatancy

Let the observed "angle of internal friction" on the macro-plane SS be ϕ, while the true angle of friction on the micro-planes T is ϕ_{crit}. Observe that as the top row of rollers slides it must also rise at angle $\Delta\phi$. In soils this phenomenon is called dilation, and it occurs with densely compacted materials which are initially well inter-locked. In Fig 2 the close-packed rollers dilate initially at $\Delta\phi_{max} = 30°$: soils contain many irregular particles of different diameters whose movements include out-of-plane components, and the maximum angle $\Delta\phi$ rarely exceeds 25°. This model of soil shearing has been likened (Bolton, 1990) to the sliding of interlocked saw-blades: see Fig 3.

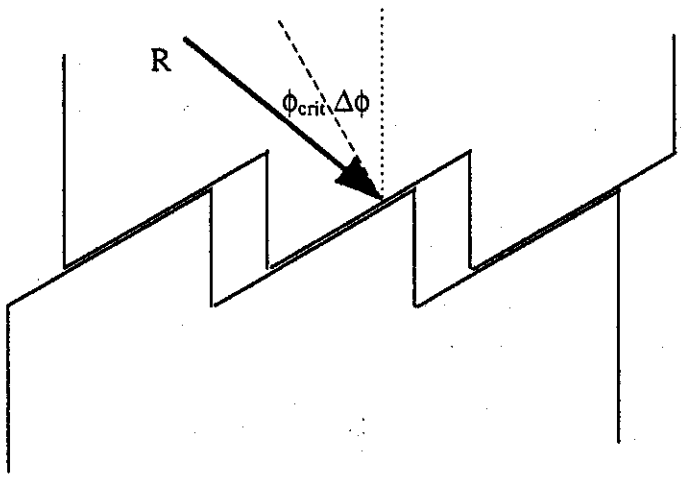

Fig 3 Friction on saw blades

In that case, comparing Fig 2 and Fig 3, we obtain

$$\phi = \phi_{crit} + \Delta\phi \qquad (7)$$

Soil shears at constant volume under particular conditions of high stress or low density known as "critical states" for which the angle of friction is regarded as a constant, ϕ_{crit}. The dilatant component of friction carries almost all the potential uncertainty for the designer since it can be as high as 25° for the densest packing of rigid angular grains, but reduces to zero if there is a reduction either in the degree of compaction or in the imposed stresses σ' relative to the fracture strength of the grains σ_f (leading to grain crushing instead of over-riding). In other words,

$$\Delta\phi_{max} = f(e, \sigma'/\sigma_f) \qquad (8)$$

Dilatancy in a disordered aggregate is irreversible (unlike the cyclic pattern which would be given after Fig 2), so it also follows that $\Delta\phi \rightarrow 0$ at large strains. "Loose" aggregates have initial $\Delta\phi < 0$ and get denser; dense aggregates have initial $\Delta\phi > 0$ and get looser. After prolonged shearing, soil attains a critical density at which it can continue to shear without further volume change. For example, it may take a granular material about 2% axial strain to reach a dilatant peak strength with some ϕ_{max}, but it will then take a shear displacement of only about 5 particle diameters on a slip plane for the internal friction to drop to ϕ_{crit} as the particles separate to a critical voids ratio to give themselves room to slide. The angle of internal friction of a soil must therefore be recognised to be a variable.

2.3 Which idealisation to use?

It is important to realise that the shear strength of soil (any soil, at any time) can be estimated either following (3) while allowing for influences such as (4), or following (5, 6) while allowing for (7, 8). It is the relative ease of making the appropriate allowances in different circumstances which has led to the short cut of reserving the word "undrained" for the short-term cohesive strength c_u of clay at constant voids ratio, and the word "drained" for the long-term frictional strength of any soil whose pore pressures are no longer a function of the loading (so that they can easily be estimated - in this case, from a hydrostatic analysis).

Following the coining of the term "effective stress analysis" to describe the treatment of soil as a two-phase material, the term "total stress analysis" came to be used for the single-phase treatment in which pore water pressures simply do not appear. It would have been much better to refer to "cohesion" and "friction" models of behaviour, as indicated in equations (3) and (6) respectively. Engineers have become confused about the fact that both models can be applied simultaneously to all soils. They let this confusion cloud their judgement regarding which model to chose in any particular set of circumstances. The art is simply to select a material idealisation whose parameter can be estimated with least uncertainty.

Any tendency for the pore water to drain externally will lead to changes of voids ratio, and therefore changes of "cohesion" which are difficult to predict quantitatively. For this reason

the drained strength of soil is almost invariably assessed using effective stresses and friction. Whenever the undrained strength of a soil exceeds its drained strength this must be due to temporary negative pore pressure increments caused by the shearing. One may think of the tendency to dilate, suppressed by inadequate inflow of water, leading to excess suction. When the undrained strength is inferior to the drained strength, positive pore pressure increments must have been induced by the shearing. One may think of grain breakage leading to load transfer onto the fluid phase. It had been thought that the latter case applies to mud, but it will be shown that *very lightly stressed* mud appears to be dilatant.

3 Undrained and drained uplift resistance

For soil cover with an average cohesion $c_{u,ave}$ we may simply re-write (2):

$$F_u = 2\,(c_{u,ave} / \gamma H)\,\frac{\left(H+\frac{D}{2}\right)}{H} \qquad (9)$$

where F_u is the undrained uplift shear factor which would be obtained for clayey soil in a particular state of prior consolidation, subjected to uplift which is sufficiently fast to nullify any effect of drainage of pore water from the zones of soil disturbance.

For soil cover with an average internal angle of friction ϕ the mechanism of Fig 1 can be interpreted directly, as in Fig 4a, or indirectly as in Fig 4b.

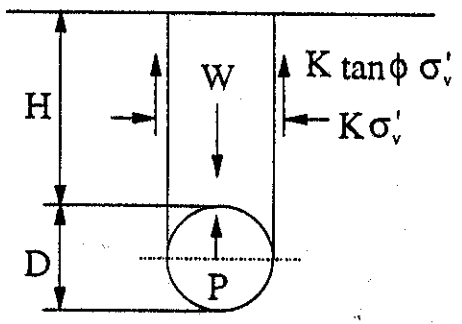

Fig 4a Frictional uplift resistance

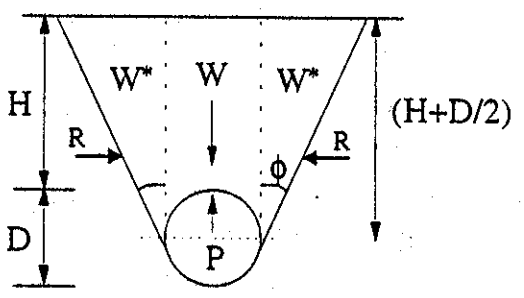

Fig 4b Dilatant uplift resistance

The frictional force on each of the vertical planes of sliding in Fig 4a is related to the angle of friction and the mean effective horizontal stress, σ'_h. This is equal to the effective vertical stress, σ'_v, multiplied by the earth pressure coefficient, K. The uplift resistance can therefore be calculated as follows

$$P = \gamma' HD + \left(H + \frac{D}{2}\right)^2 K\gamma' \tan\phi$$

Rearranged in terms of (1) this gives an expression

$$F_d = K\tan\phi \frac{\left(H + \frac{D}{2}\right)^2}{H^2} \qquad (10)$$

In Fig 4b the soil block has sides sloping upwards at ϕ so that the resultant resistance on each is horizontal, and the additional vertical resistance is represented simply by the weights W*. In order to be a viable mechanism, it is necessary to invoke an angle of dilatancy $\Delta\phi$ equal to ϕ on the side slopes, since this is the angle of the soil displacement vector (vertical) relative to the slip surface. Equation (7) shows this to be impossibly high, since there would be no inherent sliding friction at all if this were the case. Resolving vertically we obtain equation (10) again, except that in this case K = 1. The value of the alternative mechanism in Fig 4b is therefore to put an upper bound of 1 on the coefficient K which may be used in (10).

4 Sand back-fill

There is enough empirical information concerning sand back-fill for the purposes of selecting design values of density, and strength based around equation (10). For example, Schaminée et al (1990) collated data from a variety of tests on granular media which supported the following range of uplift shear coefficient F_d:

rockfill F_d = 0.9 (dense) to 0.6 (medium);
sand F_d = 0.5 (medium) to 0.4 (loose) to 0.15 (very loose).

The ranges of ϕ in these materials might be taken to be 52° to 42° for dense to medium rockfill, and 38° to 30° for medium to loose sand, respectively. Considering a cover/diameter ratio of 5 (typical of the data in Schaminee's figure), the range of coefficient K in equation (10) corresponding to these measurements would be calculated as:

rockfill K = 0.58 to 0.55
sand K = 0.53 to 0.57 to 0.22.

The most reasonable explanation is that an earth pressure coefficient $K \approx 0.55$ can be taken to act in each case, but that an extra feature caused the unusually low uplift resistance of the very loose sand. It may be hypothesised that excess pore pressures, caused by the rate of loading exceeding the capacity for drainage, or by coincidental vibrations, were responsible. In the absence of excess pore pressures, and using the lowest conceivable value $\phi = 30°$ for loose sand, with an earth pressure coefficient $K = 0.55$ fixed empirically, the lowest fully drained uplift coefficient for H/D = 5 would be $F_d = 0.38$. This coincides with the design value of $F_d = 0.4$ recommended by Schaminée et al on the grounds that the very loose sand in their study was unrepresentative of marine sandy backfills. Liquefaction or excess pore pressure generation in sandy backfill may be a concern, particularly during construction.

5 Clay backfill: case study of an Atlantic mud

The design of a pipeline to take hot hydrocarbons from sub-sea completions to a refinery on-shore provides an illuminating case study of the critical parameters in the provision of a safe cover depth to prevent upheaval buckling. A site investigation included the recovery of pairs of gravity cores, about 2 m long, at intervals of between 1 km and 4 km along the intended route. The soils were sandy close to the shore, but were otherwise clayey muds - it is these muds which call for careful testing and good judgement regarding uplift resistance.

One core from each pair was subjected to conventional soil testing:

- Atterberg plasticity tests and natural water contents;
- particle size distributions;
- quick undrained strength tests (using torvane, fall-cone and occasional unconsolidated and undrained triaxial compression tests);
- oedometer (drained compression) tests;
- drained shear box tests.

The second core was subjected to non-standard tests, more in the spirit of model tests, which were intended to simulate site conditions more closely:

- sedimentation tank tests (circa 1/5 scale) with penetrometer profiles: see Fig 5;
- uplift resistance tests (circa 1/10 scale).

Data from these various standard and non-standard tests are introduced, compared, and interpreted in the succeeding sections. The plasticity chart in Fig 6 shows the spread of Atterberg limit data, with a typical liquid limit of 70% and plastic limit of 30% giving a plasticity index of 40% (i.e. 70% minus 30%). The mud is therefore classified as clay of high to very high plasticity. A typical particle size distribution curve is shown in Fig 7; this indicates about 20% of sand-sized, 40% of silt-sized and 40% of clay-sized particles by mass. It should be noted that these distributions are obtained in the presence of a dispersing agent; the structure of the marine sediment will involve clay flocculation in the presence of sodium chloride. Sedimentation in the CUED laboratory was conducted in sea water, without dispersing agent.

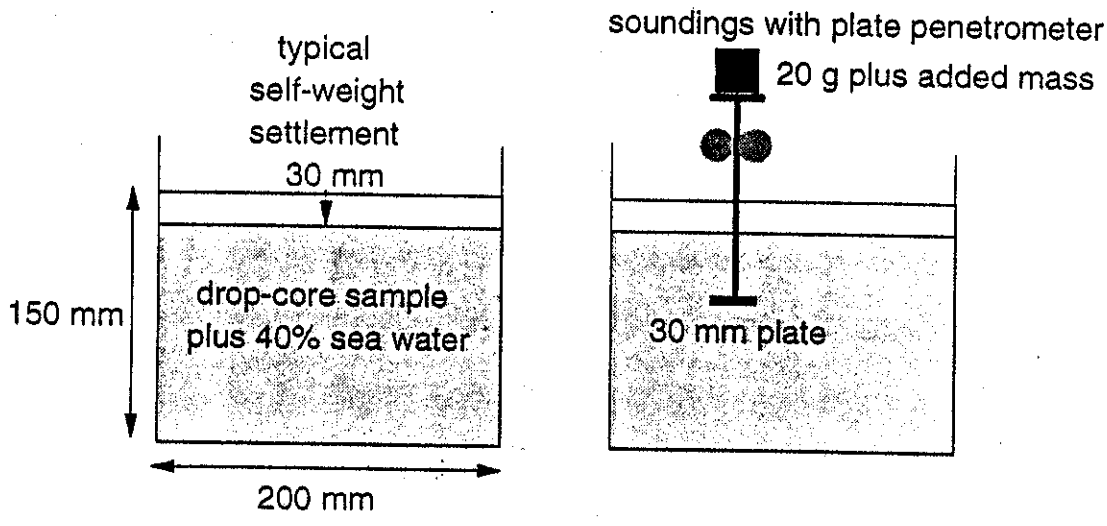

Fig 5 Sedimentation tank tests

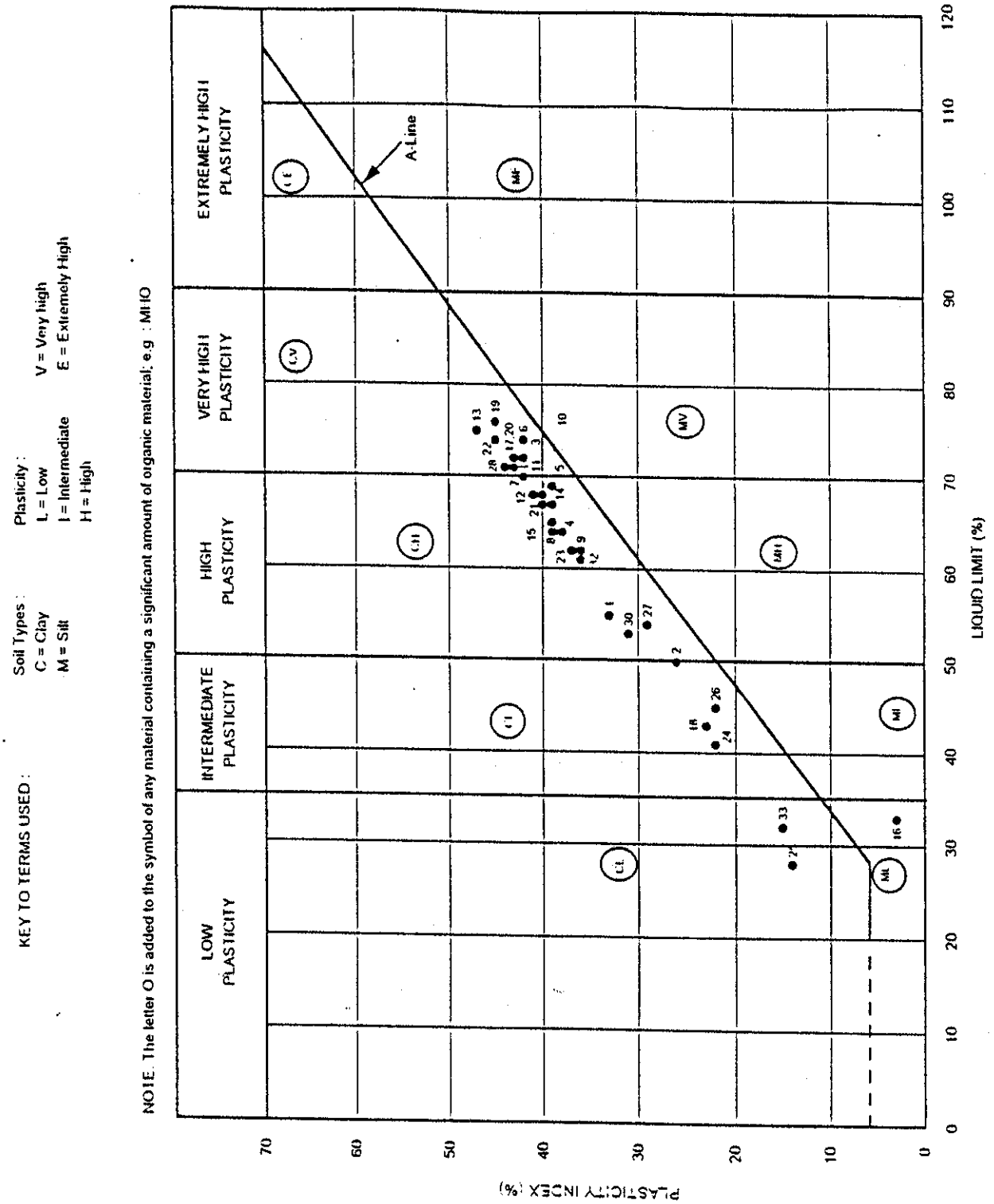

PLASTICITY CHART (BS 5930)

Fig 6 Plasticity chart for Atlantic mud

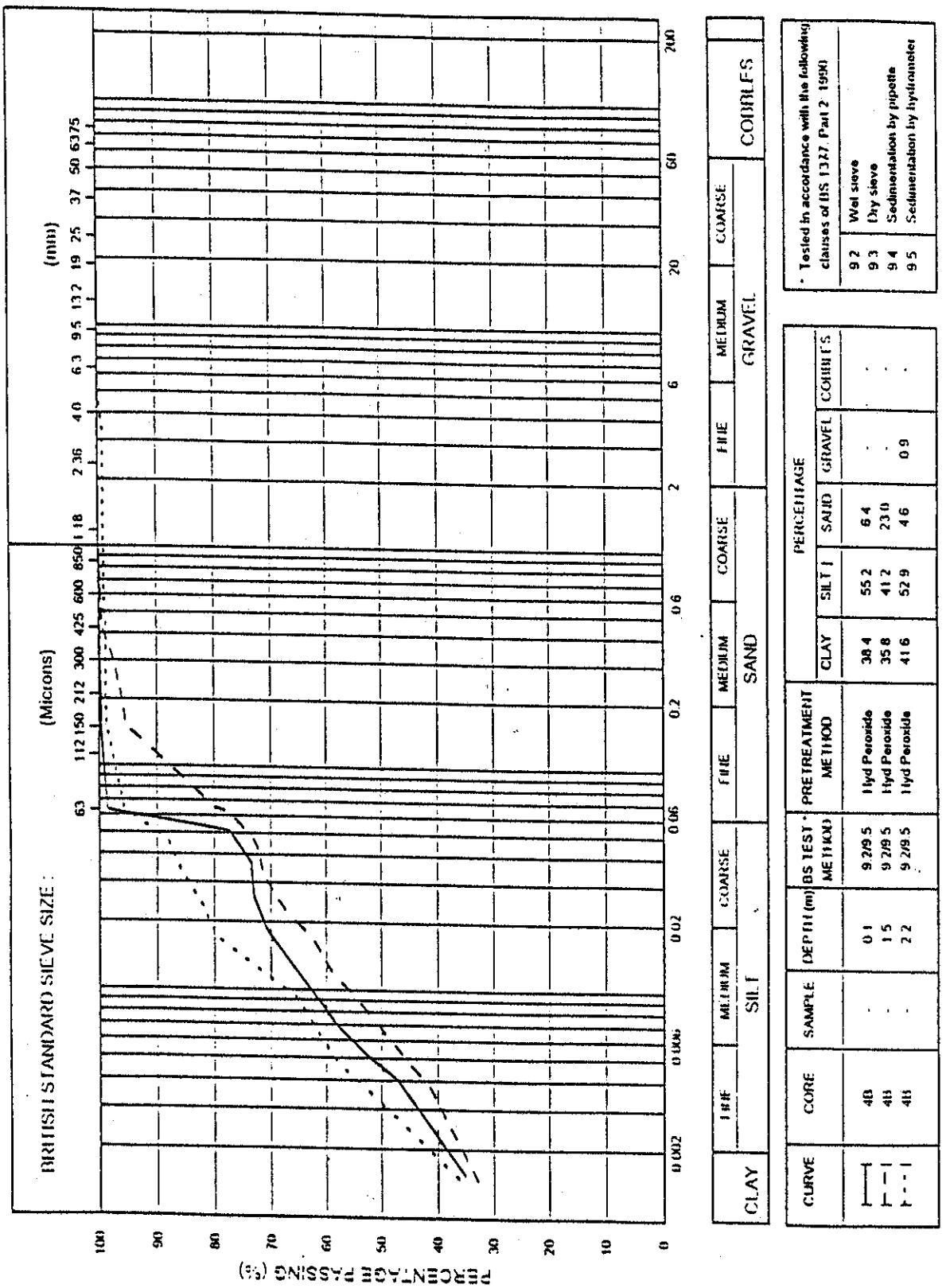

Fig 7 Typical particle size distribution for Atlantic mud

6 Density after reconstitution and reconsolidation

The machines which are used for ploughing and back-filling, or for digging-in, a pipeline will inevitably mix the natural soils with additional sea water. This reconstituted soil will fall into the space above the pipe and then will reconsolidate. The precise nature of clayey back-fills produced in this way is presently unknown; a study of marine back-fills is called for.

In this study, the clay cores at CUED were mixed with 40% extra sea water, and then placed for one hour under vacuum in a low-shear blade mixer. Any lumps which had not dispersed after that time were permitted to remain. The fluidised mixture was then permitted to reconsolidate to a depth of about 140mm (see Fig 5). More than 95% of primary consolidation had taken place after 5 days, after which the effective densities of samples from 4 particular locations along the pipeline were:

Location	2	3	5	9
γ' kN/m^3	4.1	5.4	4.3	5.4

Conventional consolidation tests on similarly reconstituted samples, mixed with additional water, and compressed to 1.7 kPa in an oedometer (corresponding roughly to the self-weight of 0.3m depth of sediment, notionally at mid-depth of the design cover) give:

Location	2	3	5	9
voids ratio e	1.72	1.88	1.83	1.67
γ' kN/m^3	6. 0	5.7	5.8	6.1

One significant observation of sedimentation in glass tanks is the typical self-inducement of heterogeneities. Fig 8 shows a typical observation for the re-sedimentation of a shelly, silty sand. The layer of finer silt settles last and traps water which may be escaping from pockets where it has been trapped. The result is the formation of internal cracks and pipes, and the formation of miniature mud volcanoes. Some cavities remain open even in the long term. In clayey mud the process is completely obscured by the cloudy water of course, and the evolution and maintenance of cracks may owe more to inter-particle forces; the end result is not dissimilar, however. Internal cracks and channels could clearly be seen in the mud even at the end of primary consolidation. The oedometer compression tests would presumably have eliminated any such features during sample preparation, and then suppressed their formation during testing due to the frictional constraint offered by the sandstone platens. This is regarded as the main reason for the reduced submerged unit weight in the former case, averaging 4.8 instead of 5.9 kN/m^3.

Another possible reason is the unrepresentatively small effective stress level in the former case. This was reviewed using the natural water contents taken from the sample cores at depths representative of the intended cover, which give an average unit weight of 5.1 kN/m^3:

Location	2	3	5	9
Depth m	0.4	0.5	0.3	0.4
w	0.77	0.81	0.93	0.78
γ' kN/m^3	5.3	5.1	4.7	5.3

Evidently, the sedimentation tests give the better guide to field values prior to construction. A design value of $\gamma' = 5.1$ kN/m^3 might be appropriate if the clay had been fully liquidised and then permitted fully to re-consolidate as cover. Clay lumps might enhance this, if present.

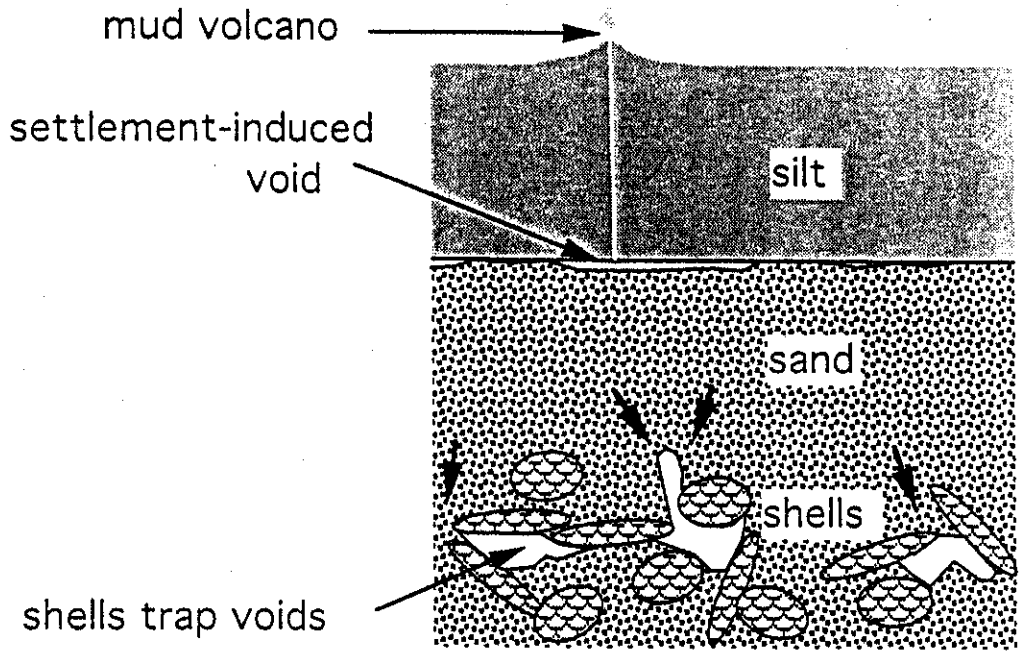

Fig 8 Heterogeneities formed during re-sedimentation of silty sand

7 Consolidation times

The rate at which water can be expelled from a soil is proportional to its permeability (hydraulic conductivity k m/s), and inversely proportional to the drainage distance (R m). The quantity which must escape due to some increase in applied stress is inversely proportional to the soil stiffness (oedometer stiffness E_o kN/m^2, where compressibility $m_v = 1/E_o$), and proportional to the layer thickness (which can be characterised by R and the boundary geometry). The time t taken to achieve some given degree of consolidation can therefore be written:

$$t = T_v R^2/C_v \qquad (11)$$

where the coefficient of soil consolidation C_v is given by:

$$C_v = (E_o k/\gamma_w) \qquad (12)$$

and the dimensionless time factor T_v can be estimated from an analysis of the transient flow process. Time for 90% consolidation $t_{90} = T_{90} R^2/C_v$ where $T_{90} = 0.85$ for simple one-dimensional compression of an isotropic layer, whereas $T_{90} \approx 0.5$ for consolidation within a V-shaped trench. Consideration must also be given to the stress distribution, and the increment which is causing consolidation. In liquidised trench fill, the increment is caused by the increase of effective vertical stress from zero everywhere towards $\gamma' z$ at any depth z, neglecting any influence of arching due to friction on the trench sides.

7.1 Data from laboratory tests

Fig 9 shows typical consolidation data of reconstituted mud tested in an oedometer. We see that the stiffness E_o = 10 kPa at σ'_v = 0.3 kPa, rising to 50 kPa at σ'_v = 2 kPa. The consolidation coefficient C_v falls from about 0.25 to 0.1 m^2/yr over the same stress range, which corresponds to a range of cover depths from 50 mm to 0.4 m.

Observations of the self-weight settlement of a 150 mm layer of reconstituted slurry, conducted in a glass tank as shown in Fig 5, are plotted in Fig 10. This typical plot shows t_{90} ≈ 75 hours. Basing the estimate on the average drainage distance of R = 135 mm, (11) gives C_v = 1.8 m^2/yr which is about 10 times faster than the rate observed at the same stress level in the oedometer.

This highly significant discrepancy was observed consistently for pairs of samples from 6 locations along the pipeline. It may be attributed to the cavities and channels which were seen to form within the mud as it settled beneath the free surface, as reported above. One extensive horizontal crack at one third the height of the sediment, if it could drain through a channel to the free surface, would theoretically reduce the drainage distance by a factor of 3, which would reduce consolidation times by a factor of 9. In the absence of an explicit measure of the internal drainage channels, such an effect would be calculated as a factor 9 enhancement of C_v. External observations through the tank walls suggested that this order of additional internal drainage was indeed taking place.

7.2 Practical significance

If precisely the same heterogeneous processes were to occur in the field as in the sedimentation tanks, with precisely the same consolidation coefficient, 90% consolidation of 0.85m of liquidised backfill would take about 2.4 months instead of the equivalent oedometer estimate of 2.4 years. It would, however, be prudent at least to reduce the assumed consolidation rate by some factor to account for the compression of voids and closure of channels at higher stresses. A reduction factor of 2.5 on C_v was observed with the oedometer samples over a stress increase by a factor of 7. If this is applied to the prediction of the behaviour of 0.85 m of disturbed clay, based on the observation of settlement in a 0.135 m layer, the modified prediction for the field is that C_v = 0.72 m^2/yr which corresponds with 90% consolidation after 6 months. The nature of the heterogeneous structure of real clay cover, following pipe burial, and the validation of a consolidation coefficient through simple laboratory tests, remains a worthwhile topic for future investigation.

7.3 Uplift resistance through partially consolidated clay cover

Since consolidation times for moderate depths of fluidised clay cover have been shown in the case of the Atlantic mud to be of the order of 6 months, it must follow that in some cases production will be under way before consolidation is close to being complete. Figure 11 shows the terms of an analysis based on a compaction front travelling a distance R′ from the base of liquidised cover in some time t. It can be shown that:

$$R' = \sqrt{(2c_v\, t)} \qquad (13)$$

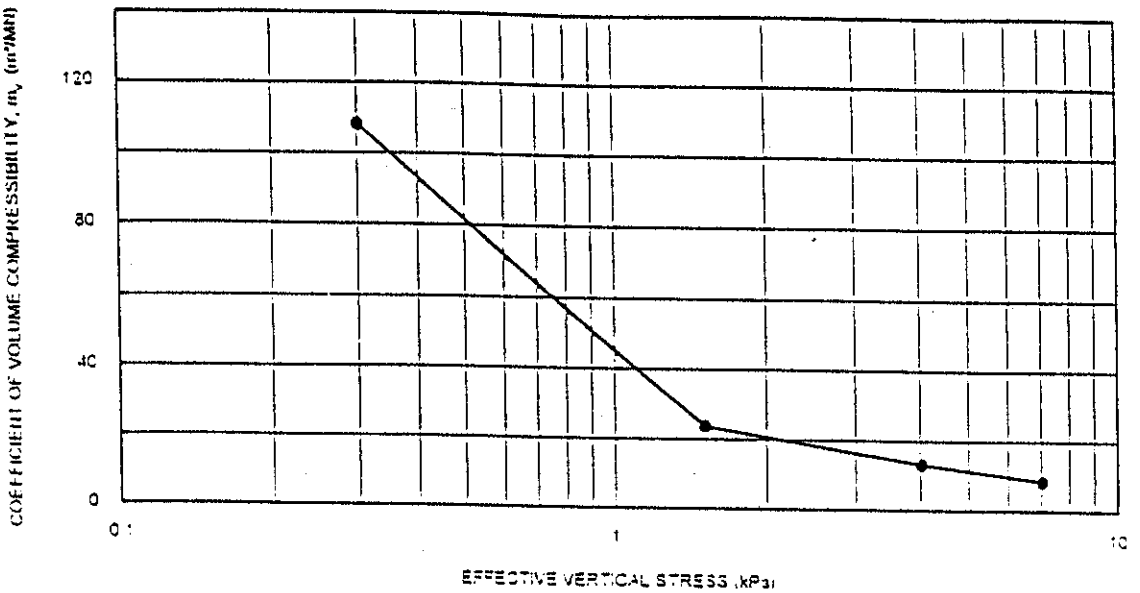

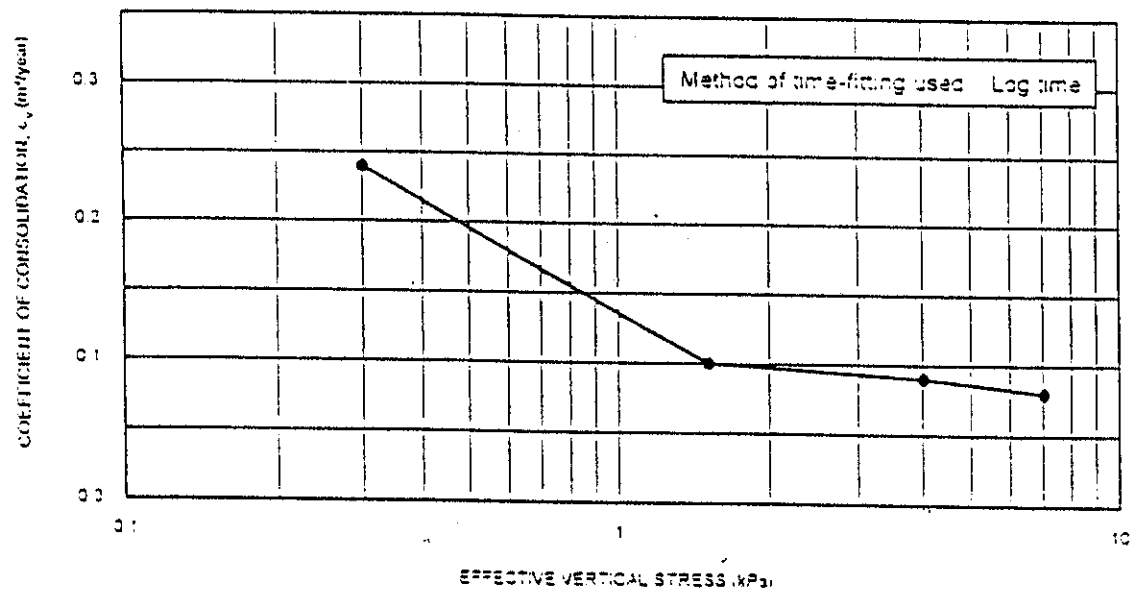

Initial Conditions					
Sample height	19.0 mm	Bulk density	1.87 Mg.m^{-3}	CORE	WCB
Sample diameter	50.0 mm	Dry density	0.90 Mg.m^{-3}		
Degree of saturation	100 %	Moisture content	74 %	SAMPLE	1
Particle density	2.70 Mg/m^{3} (Assumed)	Lab temperature	21 °C		
		Swelling pressure	N/A kPa	DEPTH m	0.8

Tested in accordance with BS 1377 Part 5 1990 Clause 3

Fig 9 Oedometer consolidation data

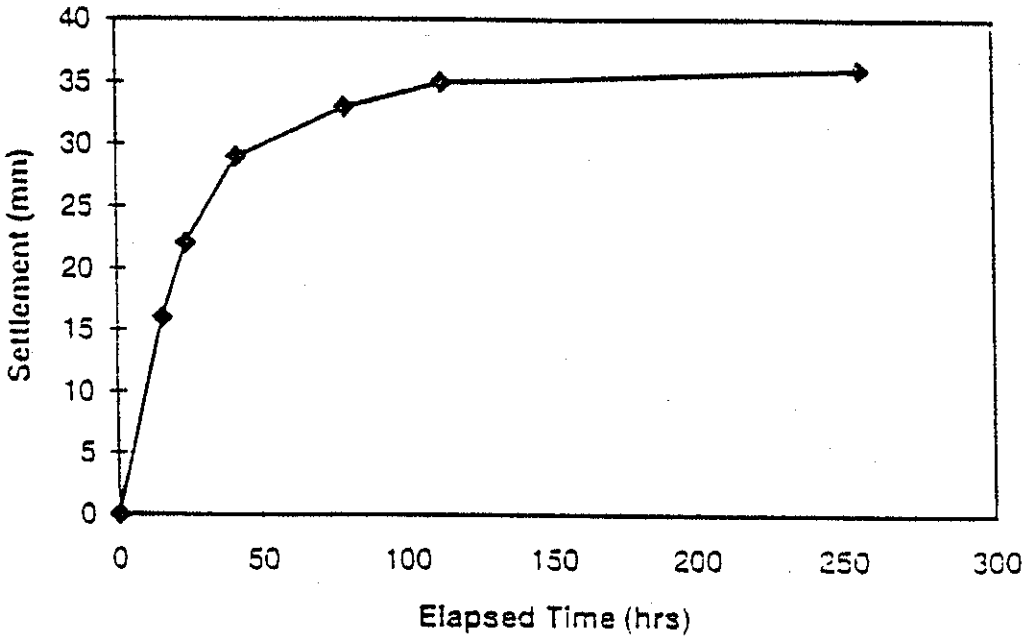

Fig 10 Self-weight consolidation data

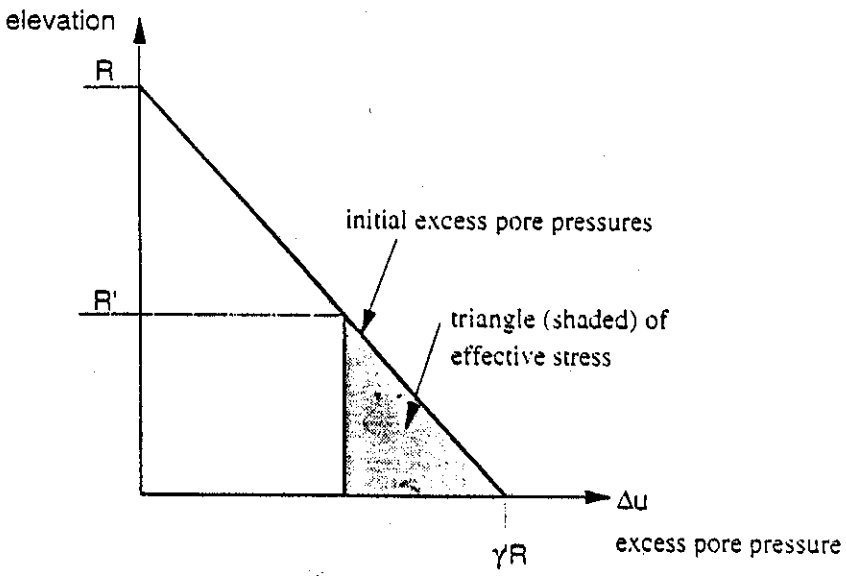

Fig 11 Consolidation of hydraulic fill: compaction front analysis

The simple basis of the compaction front idealisation is that the clay cover is treated as a hydraulic fill which is initially placed to create a triangular distribution of excess pore pressures, and that these excess pressures turn into effective stress through the advance of a compaction front. Ahead of the front the cover remains fully liquefied, and therefore completely ineffective. Behind the front there is an effective depth R' of soil with an effective unit weight γ' corresponding to the final fully consolidated soil density. The model is approximate, and predicts that consolidation is complete after a time

$$t_c = 0.5\, R^2/C_v \qquad (14)$$

This predicts that consolidation in the laboratory tanks would be complete after a time of about 4.5 days or 106 hours, which can be seen to be empirically reasonable in Fig 10.

The derivation of a partially drained uplift resistance for times $t < t_c$ can now be carried out using equation (1) replacing the cover height H by an effective cover height H′:

$$H' = R' - D' \qquad (15)$$

where D′ is the distance from the pipe crest to the base of the liquidised clay (in most cases, presumably, $D' \approx D$) and using (13) for R′. This analysis neglects volume compressibility except at the compaction front, and ignores the influence of trench geometry and the presence of the pipe on the flow regime.

It should be noted that the rate of consolidation, leading to an effective cover height H′, is to be distinguished from the question of whether the rate of upheaval is to be considered fast or slow. "Fast" upheaval will lead to the use in (9) of undrained strength c_u over the effective height H′, whereas "slow" upheaval will lead to the use of ϕ over effective height H′. It is clear that the rate of drainage of pore water around an advancing pipe, due to local gradients created by its upheaval, can be faster than the rate of drainage of the whole clay cover to the top boundary. As an approximation, we might take the time t_s to achieve locally drained shearing to be:

$$t_s = 0.5\, D^2/C_v \qquad (16)$$

by analogy with (14), and considering that the excess pressures due to uplift reduce to zero at about one pipe diameter. It would follow that at some time $t = 0.125\, R^2/C_v$ the consolidation front according to (13) would have travelled only to $H' = 0.5$ H. If the cover/diameter ratio H/D were 3 then $R/D = 4$ and we can also write $t = 16 \times 0.125\, D^2/C_v = 2\, D^2/C_v$. In this particular case the cover has had only one quarter the necessary time for it to be considered fully consolidated according to (14), but the pipe has had four times the time necessary to eliminate local pore pressures according to (16). In such a case, it might be reasonable to use a drained shearing calculation on a partially consolidated cover.

It is, perhaps, necessary to emphasise that these propositions have not yet been fully validated. Centrifuge model tests, in which small scale models are tested at correct stress levels, using a centrifuge to achieve scaled up body forces, is capable of validating the method over a wide range of soil types. Field observations of the structure of the clay cover achieved by various pipe burial technologies are also necessary.

8 Undrained strength

8.1 Natural undrained strength

Shear vane, fall cone and triaxial tests were carried out at intervals on each of the gravity cores, and these data are plotted in Fig 12 as undrained shear strength c_u versus depth. Scatter arises from: geographical trends over many kilometres, local variations (patches of over-consolidation due to erosion, differences in local plasticity at deposition, etc.), small sample sizes (presence of shells, silt partings etc.), softening due to stress relief and disturbance during transport.

The (poor) linear correlation is:

$$c_u = 2.0 + 1.33\, z \qquad (17)$$

A more conservative but reasonable correlation is:

$$c_u = 0.5 + 1.33\, z \qquad (18)$$

Note that Wood (1990) shows data and correlations suggesting $c_u / \sigma'_v \approx 0.25$ for normally consolidated clays with plasticity index 0.3 to 0.5. Since $\sigma'_v = \gamma' z$ and γ' in situ was about 6 kN/m^3 in the locations of interest, this implies

$$c_u = 1.5\, z \qquad (19)$$

which also fits the lower line in Fig 12 quite well. The question is whether we can rely on an undrained strength intercept of 0.5 kPa (or more) at zero depth.

8.2 Reconstituted undrained strength

Specially constructed plate penetrometers were used in tests on the model sediments, as indicated in Fig 5. The undrained strength was deduced from bearing capacity analysis applied to a circular plate of diameter D at depth z:

$$q_p = N_p\, c_u \qquad (20)$$

where the bearing capacity factor N_p was taken to increase from $N_o = 6$ at the surface to $N_\infty = 12$ at large depth:

$$N_p = N_o + (N_\infty - N_o)\ (z / 2D) / (1 + z / 2D) \qquad (21)$$

Fig 13 shows typical observations. The mud was lumpy and, since each penetrometer profile took a different track, random variations could not be avoided. However, some general observations are possible.

The mud needed about 5 days of consolidation to approach its full strength, as predicted by equation (14); penetration data after 24 hours consolidation was typically about 50% to 75%

of its fully consolidated value. The compaction front would have been expected to be only at half-depth after 1 day, so the strength in the top half of the sample might have been expected to be zero while that in the bottom half rose to 50% of its full value at the base. At small times, therefore, the compaction front analysis may be conservative. However, even after 10 days, the top 20mm of mud still behaved as though it were fluid, though the approximate compaction front model would have predicted that the clay was fully consolidated at that time. At large times, therefore, the analysis may be slightly optimistic. Overall, the analysis seems to perform adequately for design purposes.

The rate of increase of undrained strength with depth in consolidated clay (below the persistent slurry) is remarkable. The shear strength of the Atlantic mud rose to $c_u = 0.7 \pm 0.2$ kPa at a depth of 70mm below the apparent surface. Given greater time for primary consolidation, and a further opportunity for ageing, the strength could have increased further. This tends to support strength profile (18) as a conservative bound for the natural samples, and conflicts with the conventional understanding in (19). The possible significance of this may be appreciated by calculating $c_{u,ave}$ for a typical 0.67 m of cover; using (19) we get 0 to 1 kPa with an average of 0.5 kPa, using (18) we get 0.5 to 1.4 kPa with an average of 0.94 kPa. The design value of undrained soil strength can roughly double, if the evidence of Figs 12 and 13 can be used to infer a small but finite strength at zero depth.

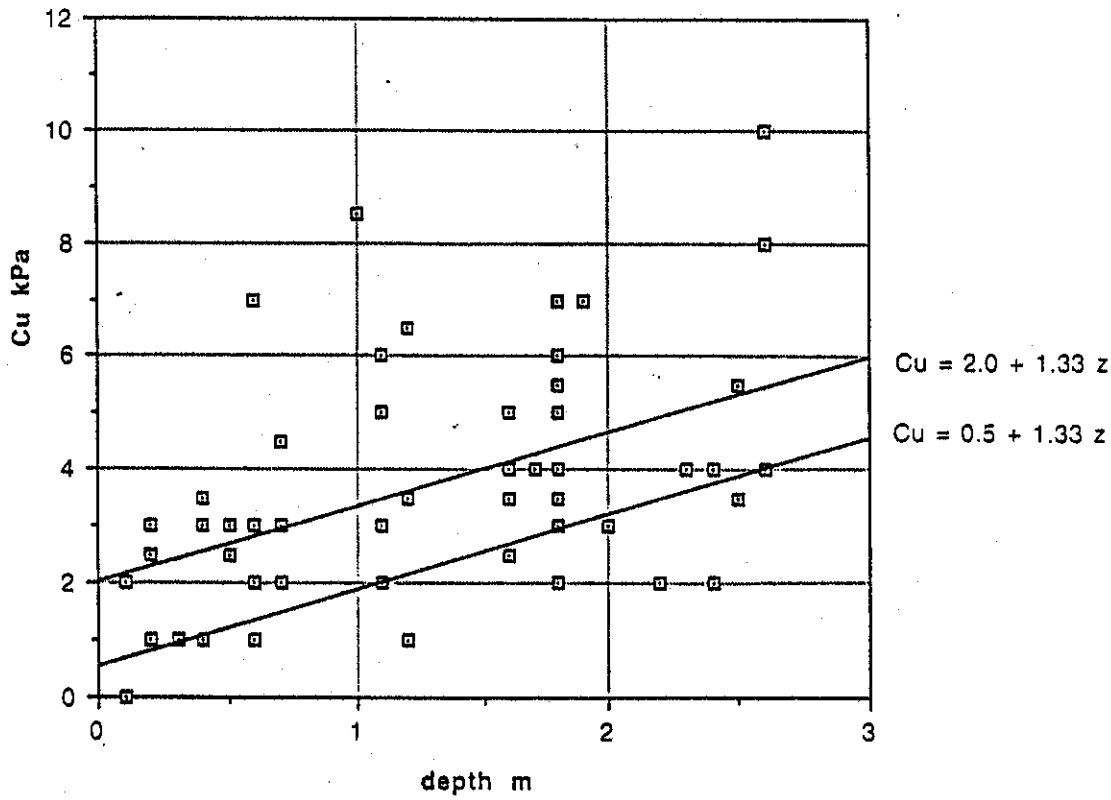

Fig 12 Natural undrained strength data

Area 8A

Penetrometer Test 13:50 19th August 1996 After 265 hrs of settlement

Total Mass (g)	Depth (mm)
0	0
20	4
30	7
70	9
120	10
170	12
220	16
350	18
400	21
500	30
550	35
600	40
640	46

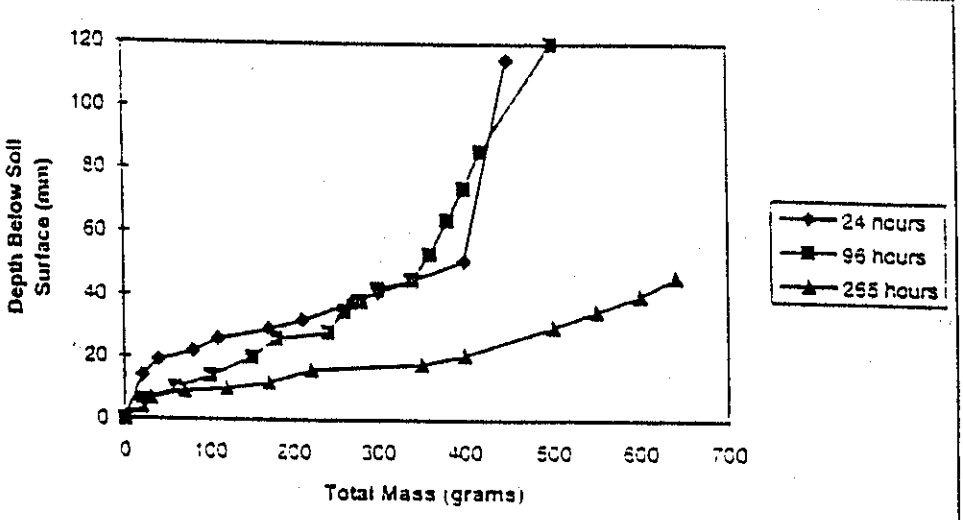

Area 8A Plot of Cu against Depth

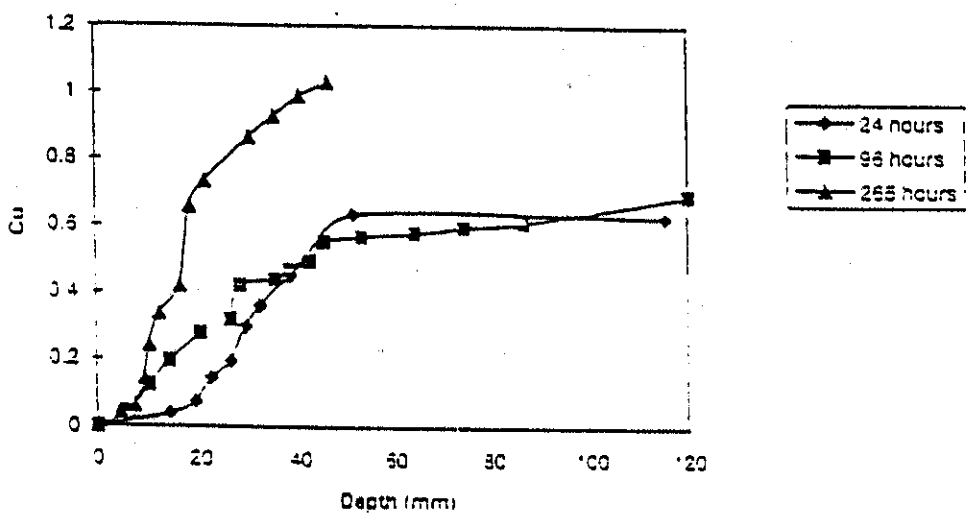

Fig 13 Plate penetrometer profiles of undrained strength in reconstituted samples

9 Frictional strength

Very slow, drained direct shear tests were carried out at CUED in 100 mm square shear boxes, under low confining stresses. The most relevant effective stress level would have corresponded to the depth of cover, e.g. up to 4 kPa at 0.67 m depth. Tests with conventional apparatus are very difficult to validate at this level; a 100 mm square sample would develop a normal force of only 40 N. Some tests were carried out at somewhat higher stresses. Some samples offered ϕ_{max} values in excess of 45° under a normal effective stress of 9 kPa; see Fig 14. This was confirmed by an independent laboratory. Figure 15 shows the friction angle mobilised at various shear displacements in the weakest material which was found along the route. Under a normal effective stress of 9 kPa the internal coefficient of friction (i.e. tan ϕ) rose to about 0.73 giving ϕ = 36°, whereas under 18 kPa the coefficient dropped to about 0.6, giving ϕ = 31°. However, it was noted that in every case the achievement of tan $\phi > 0.5$, or $\phi > 26°$, required large shear displacements (and accordingly long shear durations). This latter value, 26°, is the magnitude of ϕ_{crit} expected for a clay of this plasticity index: Wood (1990).

The larger values, developed at high relative displacements and very low effective stresses, were unexpected. One viable explanation is that clay platelets form aggregations (flocs, peds) which do not crumble when sheared very slowly under very small stresses. They therefore create internal dilation rather after the fashion of equation (7), though their very slow rate of strain-hardening up to peak strength is exceptional. In effect, the Atlantic mud can be seen as behaving rather like a crushable sand, except that the grain (floc) crushing strength appears to be just a few kPa. Evidently, it would be beneficial measure the fully drained, frictional strength of a wider variety of muds under very low confining stresses.

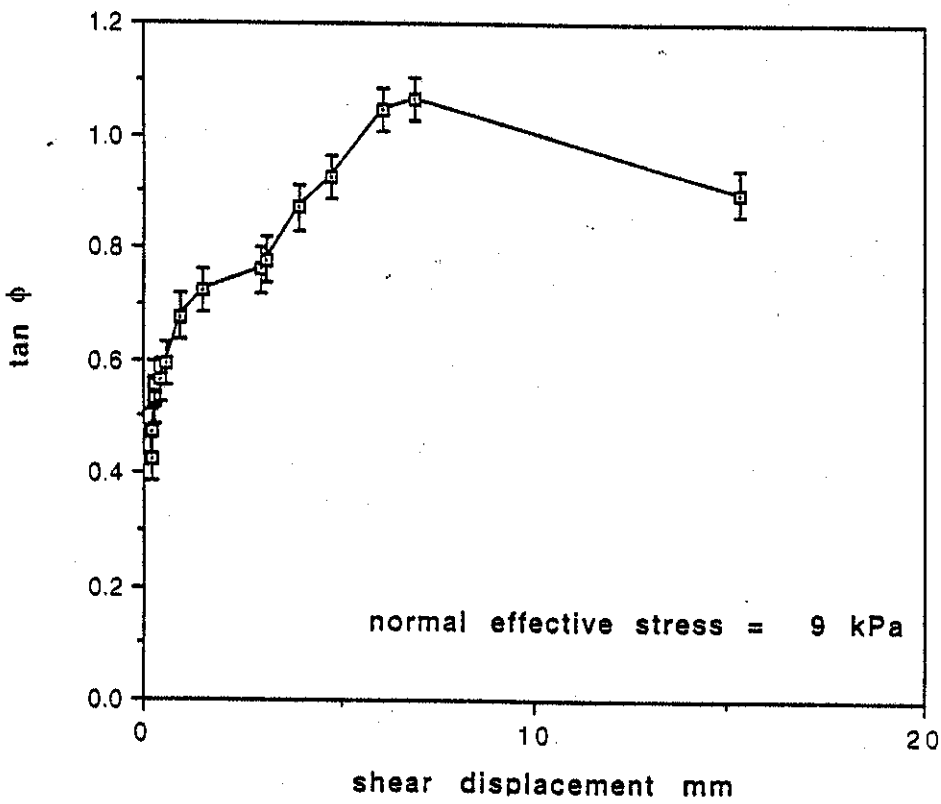

Fig 14 Drained shear box test on mud, confined under 9 kPa

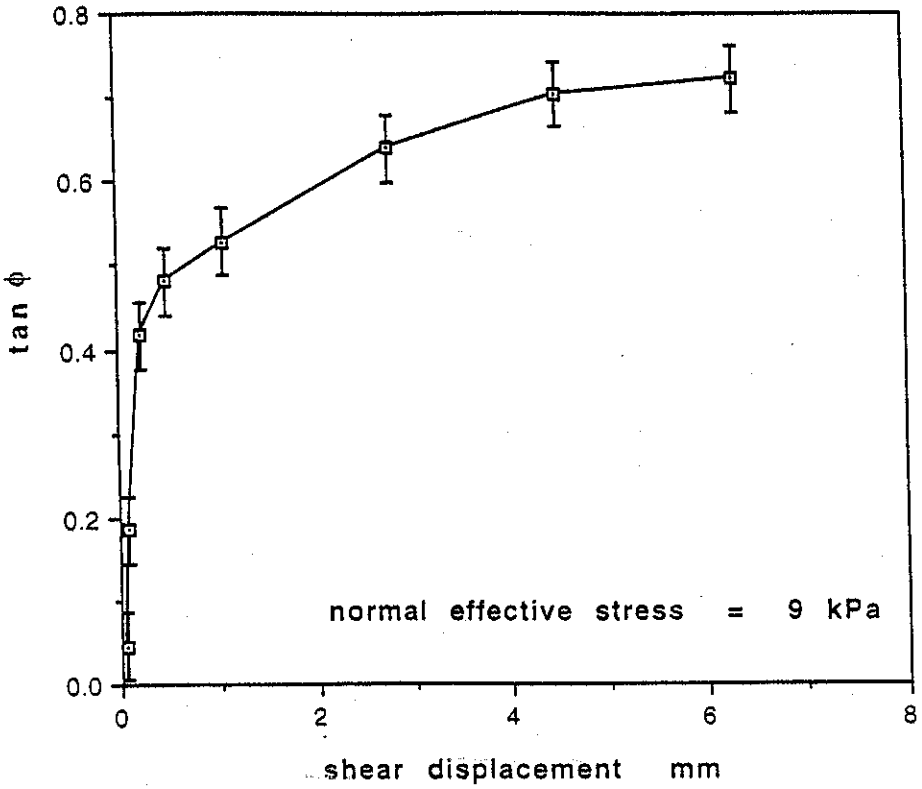

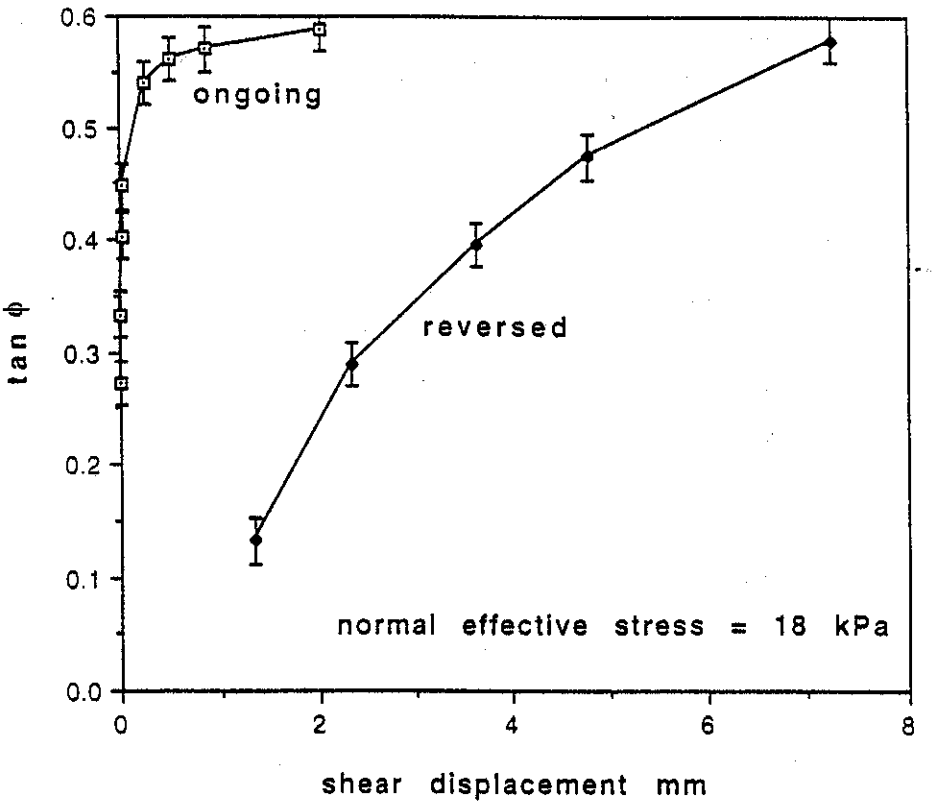

Fig 15 Drained shear box tests on mud confined under 9 kPa and 18 kPa

10 Model uplift tests

Uplift resistance was measured at small scale, and under reduced stresses, in the apparatus shown in Fig 16, in which a 1/10 scale pipe can be pulled through clay consolidated into a pre-formed "trench" in marine plywood. Clay from the cores was treated in two distinct ways prior to placement in the models. In one approach, the soil was teased by hand into pellets about 10 mm in their major dimension, which were then permitted to soften by being stored under sea water for some weeks prior to being transferred to the model. In the other approach, the clay was mechanically liquidised with excess sea water, as described in section 6 above, and permitted to re-consolidate in layers of roughly the same depth. On transfer to the model apparatus there was little noticeable difference between the two consistencies obtained, and the results were merged.

The data in Fig 17 pertain to a 20 mm model pipe with a cover of about 115 mm which had been permitted 14 days of self-weight consolidation. It was extracted in three episodes, spread over 3 days. In the first episode (up to point A on Fig 17), the rate of uplift of about 4 mm/hour was maintained for roughly 4 hours. A vertical tension crack developed above the pipe. Next day, the pipe was lifted further at a rate of 2 mm/hour for about 8 hours (point A to B on Fig 17). On the third day the rate of uplift was further reduced to about 1.5 mm/hour. There is some evidence in the data around point B that speed reduction led to a slight reduction in resistance. On the other hand, by the close of the test the pipe had risen by about 35 mm, or roughly 30% of the initial cover, so some loss of resistance should have occurred due to loss of cover. The correction for cover changes during testing is not straightforward, however, since the uplift may lead to: flow of soil around the pipe, densification of the soil immediately above the pipe, heave of the ground surface. Only the first of these mechanisms would lead to an uncompensated loss of cover.

The data in Fig 18 pertain to an identical geometry, but to clay from a different location which was permitted just under 4 days of self-weight consolidation prior to its uplift. The average rate of extraction was kept at 1 mm/hour by intermittent use of the actuator. At points A and B the very slow rate of uplift was transformed to a very fast rate of 300 mm/hour. The straightforward interpretation is that the slow extraction conforms to fully drained conditions, and the fast extraction to quasi-undrained conditions under which the resistance was almost doubled.

Fig 19 amalgamates the data from the relatively slow extraction phases of various tests, and shows the uplift shear factor F_d (calculated on the basis of nominal conditions at the start of the test) plotted against the square root of consolidation time in the model prior to uplift. The bilinear fit to the data is based on the proposition that fully drained soil required 5 days of self-weight consolidation at this scale, as reported earlier, which marks the transition to a fully drained uplift factor of about 0.9. Note that with an estimated value of $\phi_{max} = 45°$ at these very small stress levels (section 9), and H/D = 5.75, we require an earth pressure coefficient K = 0.75 in (10) to give an uplift shear factor $F_d \approx 0.9$.

The relatively high factor in test 5/1 can partially be attributed to the relatively fast rate of extraction of 5 mm/hour, which led to a characteristic vertical tension crack, with the implication that excess negative pore pressures were being induced during shearing. If the ratio $(c_{u,ave} / \gamma' H)$ is taken as 0.97, consistent with the assumption of an undrained strength profile with a linear increase through 0.7 kPa at 70 mm, (9) gives $F_u = 2.1$, which predicts an

undrained/drained uplift resistance ratio P_u/P_d = 2.1. This is consistent with the evidence in Fig 18 of a doubling of resistance at the highest rates of extraction in these small scale models.

The relatively low factors in tests 4/3, 4/4 and 4/5 can chiefly be attributed to the small consolidation times permitted prior to upheaval in each case. In particular, test 4/5 was carried out after only 26 hours after pipe burial, and generated only $P / (\gamma.H.D) = 1$. This can best be understood in terms of there being a fully drained uplift shear factor $F_d = 0.9$ working on an *effective* cover of only $H' = 40$ mm, if (1) is to be satisfied. This in turn can be related to a consolidation front which has had time to advance only about $R' = 65$ mm from the base of the trench, according to (13); this is consistent with a consolidation coefficient of 0.72 m^2/year, which is about one half that measured in the settlement tanks. In this interpretation, the upper 75 mm of clay is treated as a heavy fluid with zero resistance.

11 Scale effects

Although the recommended calculations of uplift resistance have proved reliable against the data of the 1/10 scale models, it must be recalled that the stress levels involved were similarly reduced by a factor of 10. In the light of the stress-dependence of critical parameters such as internal friction angle ϕ, consolidation coefficient C_v, and normalised mean undrained strength ($c_{u,ave} / \gamma H$), some caution is required in selecting appropriate design parameters for the field. Consider a 200 mm flowline with a fully consolidated cover of 0.6 m of Atlantic mud. Allowing for complete consolidation in the field, a design value of effective unit weight γ might be 5.1 kN/m^3. If the strength profile in (18) is thought to be conservative, the factor ($c_{u,ave} / \gamma H$) = 0.29, so the design value of the undrained uplift shear factor F_u is 0.67. If the design value of ϕ is taken quite conservatively as 26°, and the earth pressure coefficient K is also conservatively taken as 0.55, the design value of the drained uplift shear factor F_d becomes 0.37. It is likely that this is over-conservative, and that a value of 0.50 might be more appropriate, though further validation would be called for. At full scale, it is therefore anticipated that 600 mm of cover would still give slow, drained shearing as the critical design case for minimum uplift resistance - though the comparison is more marginal than it was with the models. Finally, the consolidation coefficient C_v can be taken to be about 0.72 m^2/year, but the uncertainties regarding the structure of the clay cover after pipe burial make this parameter the hardest to select, and a value 3 times smaller or 3 times higher would be believable based on the evidence of reconstituted material in the laboratory.

12 Conclusions

1. The rate of re-consolidation is critical to the development of effective clay cover. In a comparative trial, the times for self-weight consolidation of a liquidised clay slurry were an order faster than those for oedometer compression of a particular high plasticity clay. This was attributed to heterogeneities such as cracks and channels which formed beneath a free surface. It is straightforward and cheap to perform this comparison as a routine guide to better decision-making. A calculation has been proposed which incorporates the consolidation coefficient into a calculation of the time required for the cover to become effective after pipe burial. However, the degree of water-entrainment in the field, with the variety of pipe burial technologies which may be employed, is unknown. The structure of typical clay covers, and the observation of their rates of consolidation, is of vital interest.

2. The uplift resistance of soil cover can best be interpreted in terms of an uplift shear factor, which has been shown to be proportional to the operative shear strength of the cover. The design value of the fully drained uplift shear factor is likely to be smaller than the normalised undrained factor for moderate clay covers, but both fast and slow shear mechanisms should be checked. The undrained strength of mud at very shallow depths has been seen to exceed that expected of "normally consolidated" soils by a large factor. This is attributed to temporary excess negative pore pressures induced by shearing the mud, which behaves like a dilatant material within the first metre of cover in the case of the mud reported here.
3. The use of a critical state friction angle will be conservative in the calculation of the drained strength, but it may be over-conservative. In the particular case of the high-plasticity Atlantic mud it would seem acceptable to design with an uplift shear factor of 0.4, which would previously have been thought applicable to medium-dense sands. However, work on frictional resistance measured at the correct stress levels in the field may lead to the validation of substantially higher strengths, closer to the value of 0.9 which was observed in small-scale, reduced-stress, models.
4. It will be possible to perform centrifuge tests on reconstituted soil from gravity cores, so that small-scale models can be tested at field-scale stress levels, thereby avoiding the need for overt conservatism. This should provide an economic and reliable way of obtaining all the critical design parameters. Different consolidation times, and both fast and slow uplift tests, can be conducted. This will overcome the evident deviation between the real behaviour of muds and the assumed behaviour described in textbooks. At the same time, the problem of geographic variability will largely be solved if new test methods are developed which can be applied to individual gravity cores.

13 References

Bolton M.D. (1991) A Guide to Soil Mechanics, 439 pp, published by M.D.&K.Bolton, 232 Queen Edith's Way, Cambridge, CB1 4NL, UK.

Schaminee P.E.L., Zorn N.F. and Schotman G.J.M. (1990). Soil response for pipeline upheaval buckling analyses: full-scale laboratory tests and modelling, OTC 6486.

Wood D.M. (1990) Soil Behaviour and Critical State Soil mechanics, 462 pp, C.U.P.

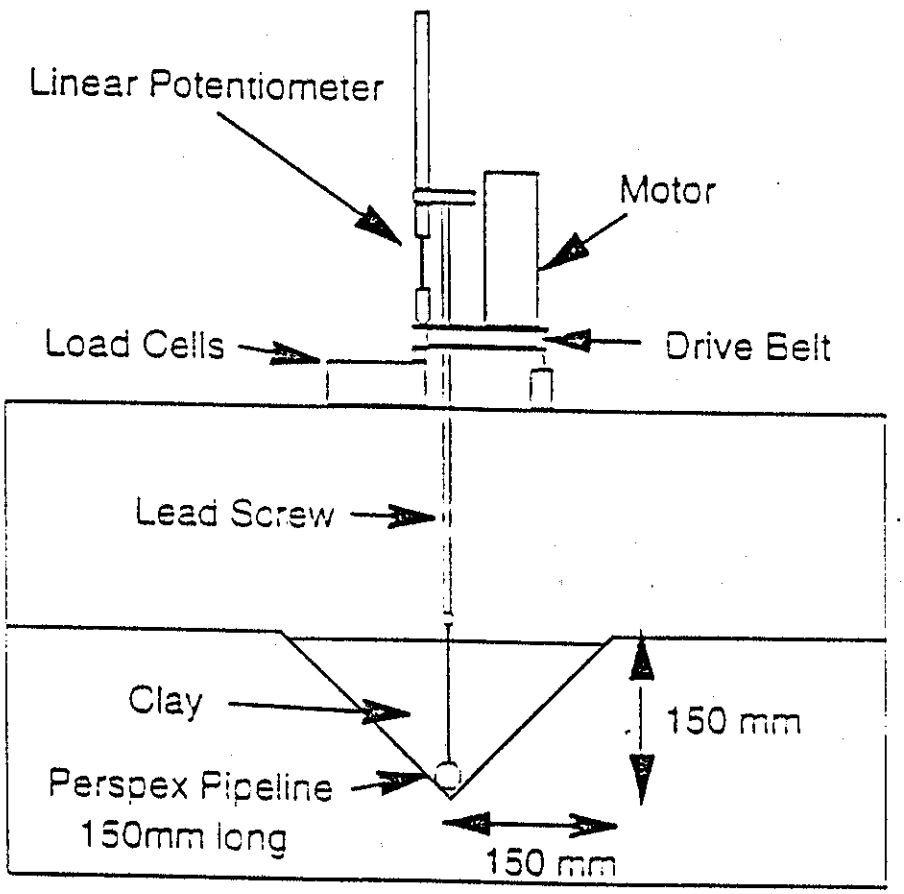

Fig 16 Model uplift resistance test rig

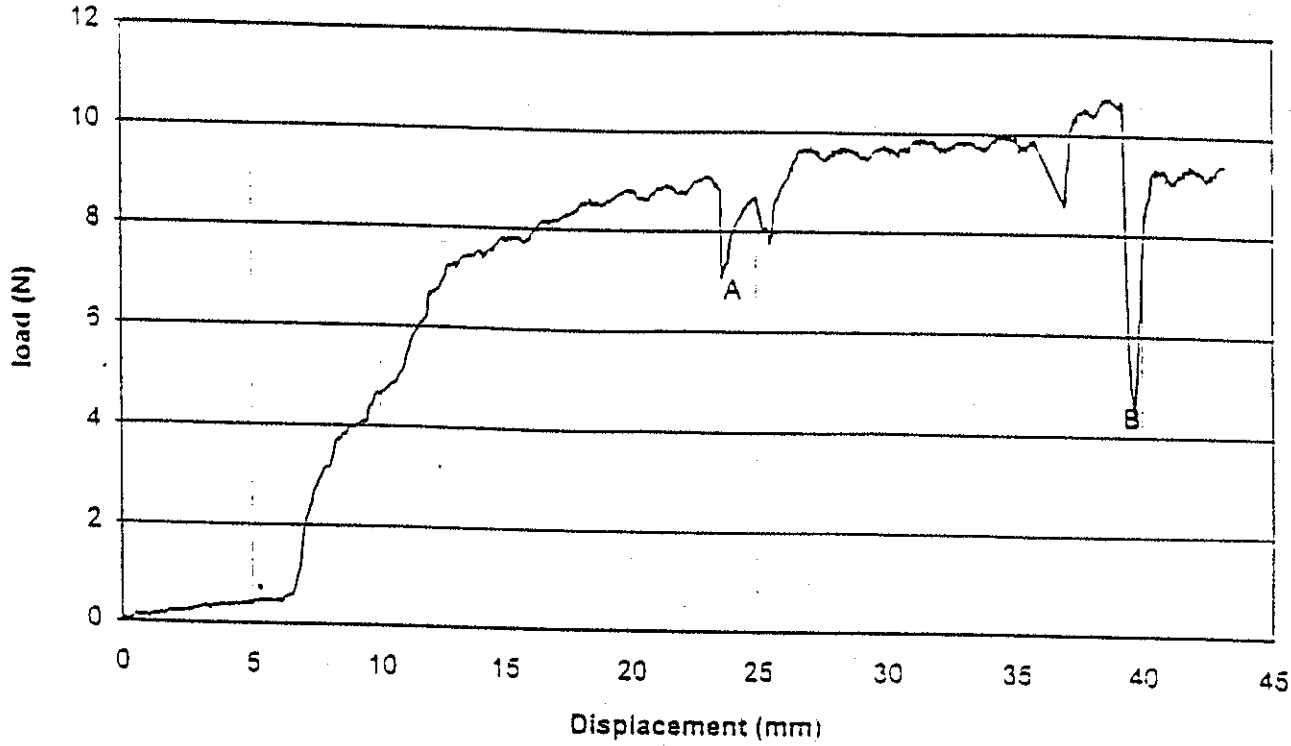

Fig 17 Uplift resistance versus displacement; 14 days' consolidation

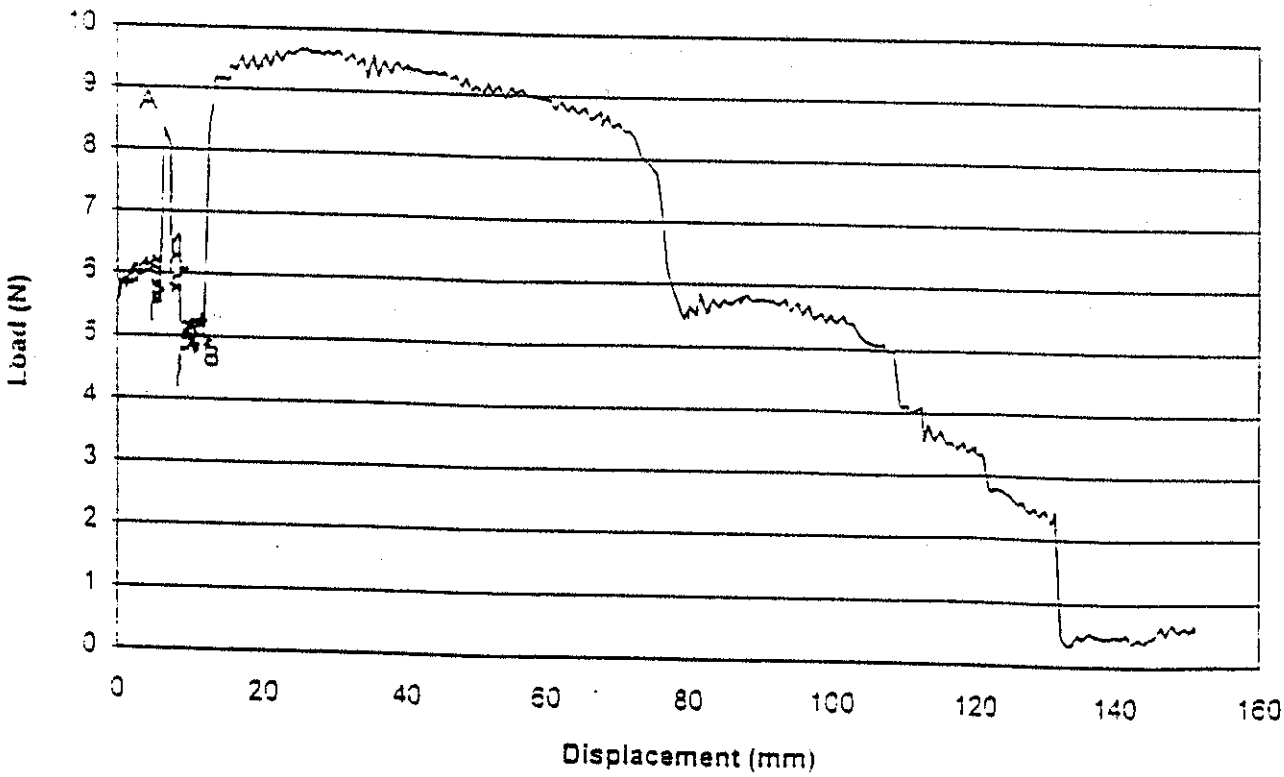

Fig 18 Uplift resistance versus displacement; 4 days' consolidation

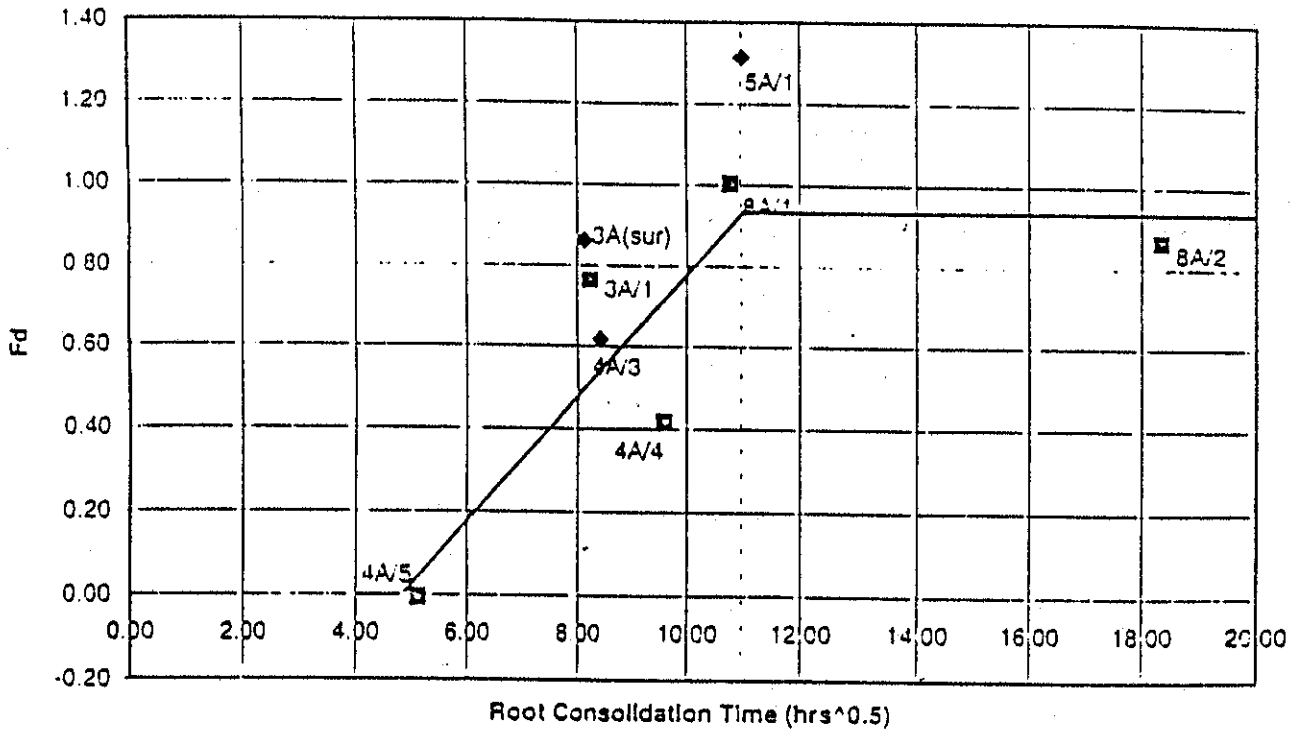

Fig 19 Drained uplift shear factor F_d, versus root consolidation time